applied sciences

MDPI

Article

Assessing VOC Dispersion from Hydrocarbon Storage Tanks: A Case Study on Emission Temporal Resolution

Francesca Tagliaferri *, Selena Sironi and Marzio Invernizzi

Materials and Chemical Engineering "Giulio Natta", Department of Chemistry, Politecnico di Milano, Piazza Leonardo da Vinci 32, 20133 Milano, Italy; selena.sironi@polimi.it (S.S.); marzio.invernizzi@polimi.it (M.I.)
* Correspondence: francesca.tagliaferri@polimi.it

Abstract

Volatile Organic Compound emissions from hydrocarbon storage tanks are a key source of industrial air pollution and odour nuisance. This study evaluates odour impact predictions using annual average emissions versus time-resolved emissions from fixed roof tanks and external floating roof tanks that store different hydrocarbon products, including crude oil and refined products such as gasoline, diesel, kerosene, fuel oil, and bitumen. Odour emission rates are derived from field measurements and laboratory data and implemented in CALPUFF dispersion modelling. The results show that for fixed roof tanks, time-resolved emissions predict odour separation distances up to four times greater than annual averages, with central domain differences reaching 300% and boundary variations between 50–100%. In contrast, floating roof tanks show minimal variation (<10%) between the two methods. These findings highlight that odour perception is driven by short-term peaks rather than long-term averages and that using annualized emissions may significantly underpredict odour impacts, especially for fixed roof tanks. Accurate temporal characterization is thus essential for realistic odour assessments and effective regulatory compliance.

Keywords: dispersion modelling; CALPUFF; hydrocarbon storage; odour emission; tanks; VOCs

1. Introduction

Volatile Organic Compound (VOC) emissions from Oil & Gas operations represent a significant source of industrial air pollution, impacting air quality and the environment around these facilities [1–4]. For instance, refineries, which process crude oil into various petroleum products, release a variety of VOCs during different stages of production, including storage, transfer, and processing [5,6]. Petrochemical plants also use hydrocarbons for the production of specific organic molecules [7,8]. These emissions not only contribute to the formation of ground-level ozone and smog but may also impact local communities through odorous compounds that can affect the quality of life [9–12].

Combustion processes, such as those in boilers, heaters, and flares, release odorous sulfur compounds and other VOCs. Likewise, product loading and unloading operations contribute to odour emissions due to the handling and transfer of raw materials and refined products. Wastewater treatment within Oil & Gas facilities also generates VOC emissions, as inlet water may contain sulfur compounds and other volatile substances with a high odour potential [13–15]. Understanding the dynamics of VOC emissions is crucial for effective regulatory measures and public health protection [16,17].

Academic Editor: Regina Duarte

Received: 12 January 2026
Revised: 10 February 2026
Accepted: 11 February 2026
Published: 12 February 2026

One of the most significant sources of odorous emissions in the Oil & Gas sector is the storage and handling of crude oil and refined products [18–20]. These storage tanks are designed to store volatile materials, and due to temperature fluctuations, pressure changes, and handling activities, VOCs can be released into the atmosphere. There are two main types of storage tanks that may release VOC in the atmosphere: Fixed Roof Tanks (FRTs) and External Floating Roof Tanks (EFRTs).

FRTs, characterized by their static, immovable roof, create a confined gaseous headspace above the liquid product, where vapours can accumulate. As the tank is filled and the liquid level rises, the vapour space is compressed, forcing the release of VOCs through vapour displacement. This process, known as "working losses", represents the primary emission contributor [14,21]. In addition, FRTs also experience emissions due to "standing losses", essentially caused by the daily thermal cycle. These losses occur when temperature changes cause the vapour in the tank to expand and contract, releasing small amounts of VOCs [22]. According to Invernizzi et al. [13], standing losses are a minor contributor to operational FRTs to total emissions, compared to working losses.

In contrast, EFRTs are designed to minimize vapour accumulation by featuring a movable roof that floats directly on the liquid surface, thereby reducing the headspace and limiting the potential for vapour formation. However, these tanks are not completely sealed, and VOC emissions can still occur at the points where the floating roof meets the tank wall, known as "rim seal losses", as well as at various openings and fittings on the roof, such as manholes and vents, referred to as "deck fitting losses". Both types of emissions are influenced by temperature and pressure fluctuations, which can cause minor movements of the roof or create small gaps, allowing VOCs to escape. Additionally, working losses in EFRTs arise when the roof moves downward due to the film of liquid adhering to the tank walls. As the liquid evaporates, this leads to the displacement of vapour and, consequently, VOC emissions [23–26].

Numerous studies have investigated VOC emissions from hydrocarbon storage tanks, primarily focusing on their contribution to air pollution and their environmental impact on surrounding areas [24,27–31]. However, research specifically addressing odour emissions from these tanks is extremely limited. The few existing studies on hydrocarbon-related odour emissions generally focus on either methodology for estimating emissions [13,14], without addressing atmospheric dispersion, or modelling approaches to assess the impact of an entire site [32–34]. To date, the odour impact of storage tanks as individual sources has not been systematically evaluated, despite their potential contribution to odour nuisance in nearby communities.

In the context of odorous gas emissions, it is essential to recognize that the concentration of a substance advected by a turbulent boundary layer flow often exhibits substantial fluctuations around its mean value [35]. Unlike traditional air pollutants, which are typically regulated based on long-term average concentrations, odour impacts are primarily assessed using short-term peak concentrations and percentiles [36,37]. This difference is key, as odour nuisance is a transient phenomenon driven by brief, high-concentration spikes, rather than continuous exposure. As such, a more granular approach to emission input data is necessary to capture these peaks, which are crucial to understand odorous emissions and their impact. This is particularly significant for hydrocarbon storage tanks, which display a discontinuous emission pattern, characterised by sporadic yet intense release events throughout the year, that can lead to odour nuisance. Consequently, relying solely on a constant annual emission rate may obscure critical information about odour impact on receptors, with the risk of underestimating the peak events that define actual odour perception and possible nuisance [38–40].

This study aims to quantify the odour impact of oil refinery storage tanks, leveraging high-resolution temporal emission data to improve the accuracy of odour dispersion modelling. By comparing odour impact predictions obtained using annual average emissions versus temporally resolved emissions, this study highlights how different approaches to emission characterization can lead to significantly different outcomes. The Odour Emission Rates (OERs) used in the simulations are derived from real measurements collected through field campaigns at industrial sites (for FRTs) or laboratory experiments (for EFRTs).

The simulations were performed using the CALPUFF dispersion model, selected due to its widespread application in regulatory frameworks [41,42] and its recognition by agencies such as the US-EPA [43,44]. CALPUFF's capacity to incorporate temporally and spatially resolved emission data and its ability to handle non-steady-state conditions and simulate short-term odour peaks make it particularly appropriate for evaluating the variability and intensity of odour nuisance events [45–49].

This study advances the estimation of odour emissions from hydrocarbon storage tanks, extending existing research on the influence of temporal variability in emission rates on odour impact assessments. Previous works have demonstrated that assuming constant emissions may lead to underestimation of impact areas [38,49,50]. However, these studies focused on generic modelling scenarios or agricultural sources, whereas no research has yet examined this aspect for odorous emissions from Oil & Gas operations.

In this context, the present work provides a novel contribution by applying the concept of temporally resolved emissions to industrial hydrocarbon storage tanks, where odorous releases are highly intermittent and process-dependent, and by distinguishing between FRTs and EFRTs, which exhibit markedly different emission dynamics. The study provides a quantitative comparison of how predicted odour impacts vary between these two tank types when using emission data with different temporal resolutions, thus illustrating the extent to which simplified, time-constant approaches can distort the assessment results.

2. Materials and Methods

2.1. CALPUFF Model

CALPUFF [51] is an advanced three-dimensional, non-stationary Lagrangian puff dispersion model, designed to simulate the atmospheric transport and dispersion of pollutants, including gases, aerosols, and particulate matter. It is particularly suited in case of complex orographic terrain and coastal influences.

The model simulates pollutant dispersion through discrete puffs, each containing a fraction of the total emission mass. As they travel, these puffs expand horizontally and vertically from the plume's centerline, following a normal distribution according to Equations (1) and (2):

$$C(x,y,z) = \frac{Q}{2\pi\sigma_x\sigma_y} g \left[\exp\left(-\frac{1}{2}\left(\frac{d_a}{\sigma_x}\right)^2\right)\right]\left[\exp\left(-\frac{1}{2}\left(\frac{d_c}{\sigma_y}\right)^2\right)\right] \quad (1)$$

$$g = \frac{2}{\sigma_z\sqrt{2\pi}}\sum \exp\left[\frac{-(H_e + 2nh)^2}{2\sigma_z^2}\right] \quad (2)$$

where C [g/m^3] is the concentration at (x, y, z); Q [g] is the pollutant mass; σ_x, σ_y, and σ_z [m] are the Gaussian distribution standard deviations in the along-wind, cross-wind, and vertical directions; d_a and d_c [m] indicate the distances from the puff barycenter to the receptor in the along-wind and cross-wind directions; H_e [m] is the puff barycenter's height relative to the ground; h [m] is the mixing-layer height; g [m^{-1}] is the vertical component of the Gaussian formulation, including the effects of ground and inversion layer reflections; and n is an integer index accounting for multiple reflections in the vertical direction.

CALPUFF can account for various meteorological phenomena, including variations in wind speed, direction, and atmospheric stability. The meteorological fields required by CALPUFF are provided by CALMET [52], a diagnostic meteorological preprocessor that integrates local and regional data, such as terrain information, observational data, and weather forecast outputs. CALMET generates high-resolution wind, temperature, and stability profiles to simulate pollutant dispersion under a variety of conditions.

Moreover, it also includes options for simulating pollutant removal processes, like dry and wet deposition, as well as the plume rise phenomenon. It offers flexibility in simulating plume rise by providing different algorithms, including the empirical Briggs formulation and a numerical plume rise method.

2.2. Site Description and Meteorological Data

All simulations were performed using CALPUFF version 7.2.1 on an annual basis, with a time step of 3600 s.

Chemical transformation processes were not activated, as commonly assumed in odour dispersion modelling, where pollutants are treated as chemically inert. Dry and wet deposition processes were also not included; this assumption is conservative with respect to predicted ground-level concentrations. Building downwash effects were not considered.

The dispersion option MDISP was set to 2, whereby horizontal and vertical dispersion coefficients are determined on the basis of micrometeorological parameters provided by the meteorological preprocessor, allowing for a physically based representation of atmospheric turbulence and stability effects.

Default CALPUFF values were adopted for the minimum size of newly generated puffs, with SYMIN = SZMIN = 1.

The computational domain is located in northern Italy (SW corner: 487.632 km UTM E, 4997.350 km UTM N, UTM zone 32), covering an area of 6 km $\times$ 6 km, with a grid resolution of 100 m. This area is characterized by relatively flat terrain, with an average elevation of approximately 90 m above sea level. The land use data used for the simulation were sourced from the CORINE CLC 2018 (100 m resolution) land cover database, while the terrain elevation data were obtained from the SRTM Global (30 m resolution) dataset.

To generate the three-dimensional wind field for the simulation, the meteorological data used as input for the CALMET (version 6.5.0) simulations, including both surface and upper-air data, were derived from hourly 3D outputs of a prognostic WRF model with a 1 km resolution. Unlike data from a single monitoring station, which provides only point measurements, this approach delivers spatially resolved, three-dimensional data. The dataset spans the entire year of 2022, selected as the reference period.

Figure 1 illustrates the annual wind rose (blowing-from) at the first vertical layer, 10 m above ground level, and the frequency distribution of stability classes, as extrapolated from the CALMET simulations at the centre of the domain (490.632 km UTM E, 5000.350 km UTM N, UTM zone 32). The meteorological simulation indicates prevailing wind directions from the northeast and southwest, with an average wind speed of approximately 2.84 m/s. Furthermore, nearly one-third of the annual hours are associated with stability class F, reflecting highly stable atmospheric conditions. These findings are consistent with the typical climate of the Po Valley, where the domain is located. In the CALMET/CALPUFF modelling system, calm-wind conditions are defined as situations in which wind speed is lower than 0.5 m/s. Under such conditions, CALPUFF is able to simulate stagnant puffs that are not transported by wind advection while still allowing for dispersion driven by atmospheric turbulence. This capability is particularly relevant for the simulation of odour dispersion under stable and low-wind conditions.

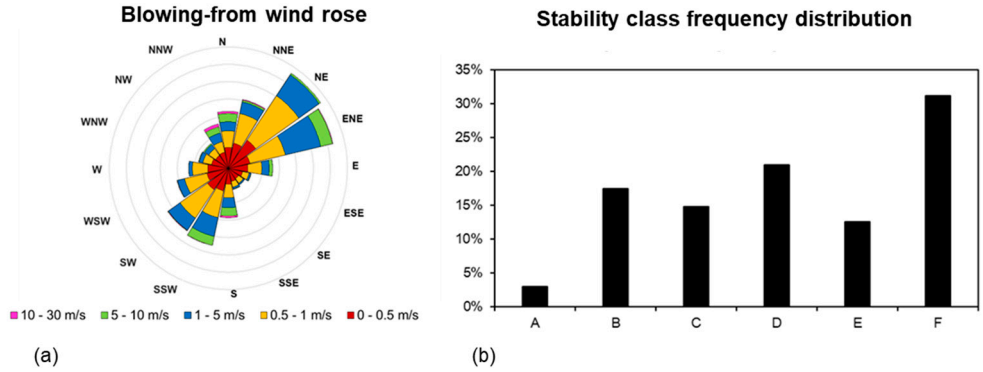

Figure 1. Annual wind rose (blowing–from) at the centre of the domain (490.632 km UTM E, 5000.350 km UTM N, UTM zone 32), (**a**). Annual distribution of stability classes, (**b**).

2.3. Emission Data and Sources Characterization

For FRTs, the OER for each tank was estimated as described by Invernizzi et al. [13], by associating the odour concentration [ou_E/m^3] representative of the stored product to the airflow [m^3/h] emitted from the tank vent during the filling phase, as working losses are the primary source of emissions for this type of tank. The model refers to freely vented tanks, i.e., not connected to vapour recovery units, flares, or vapour balancing systems, thus assuming direct venting to the atmosphere:

$$OER[ou_E/s] = \frac{Q_{air}\ [m^3/h] \times C_{od}\ [ou_E/m^3]}{3600\ s/h} \quad (3)$$

where Q_{air} is the emitted airflow during the filling phase and C_{od} is the odour concentration at the vent.

Odour concentrations for each product were obtained by averaging datasets of values collected during multiple olfactometric campaigns conducted by the Olfactometric Laboratory of Politecnico di Milano at the vents of FRTs containing different hydrocarbon products. The experimental procedures were carried out in accordance with recognized olfactometric standards [53], ensuring consistency and reliability of the measurements within the context of this study. It should be noted that these values are specific to the sampling campaigns and reflect the operational conditions of the tanks and facilities at the time of sampling, including factors such as product temperature and filling level; therefore, they should not be considered as universally applicable reference data.

A total of 21 odour concentration measurements were available for bitumen tanks, while 42 measurements were collected for the remaining refined products (kerosene, diesel, and fuel oil). For each product category, representative mean values and standard deviations of the odour concentration were computed and are reported in Table 1.

Table 1. Input for emission estimates for FRTs and EFRTs.

	FRTs	**EFRTs**
	$Q\ [m^3/y] = 7 \times 10^6$ C_{od} [ou_E/m^3]	VOC losses [kg/y] = 52,000 HCOEC [ou_E/kg]
Fuel oil	60,000 ± 69,000	-
Bitumen	150,000 ± 98,000	-
Gasoline	-	10^6
Kerosene	60,000 ± 69,000	10^7
Diesel	60,000 ± 69,000	10^7
Crude oil	-	10^8

Q = annual throughput; C_{od} = Odour concentration.

Odour concentration values showed substantial variability across tanks and monitoring campaigns, mainly related to product characteristics such as sulfur content and degree of refining. A clear distinction was nevertheless observed between bitumen and the other refined products, with bitumen consistently exhibiting higher odour concentrations, while kerosene, diesel, and fuel oil displayed broadly comparable levels. On this basis, bitumen was treated as a separate category, and the remaining refined products were grouped together in the analysis.

The airflow rate was estimated based on the hourly fluctuations in the tank level, which were obtained from a real-case refinery's DCS (Distributed Control System), resulting in an hourly variable OER throughout the year. Emissions were set to zero when the tank was in a stationary or descending phase, as emissions are associated with the loading phase, during which gas or vapor is released due to filling and pressure variations inside the tank. Additionally, a constant OER was also considered for the entire year. This was derived by replacing the hourly variations in tank throughput, as estimated from hourly level data, with the total annual throughput distributed evenly across the year, as commonly done by yearly VOC inventories [54].

In the time-resolved approach, the hourly variability of FRT emissions originates solely from the airflow rate Q_{air}, while odour concentrations are assumed constant over time and depend only on the type of product stored, thus differing from tank to tank.

In particular, the simulation of FRTs includes a total of 47 tanks, categorized as follows: 10 bitumen tanks, 5 kerosene tanks, 11 diesel tanks, and 21 fuel oil tanks.

In the case of EFRTs, the OER was derived by associating the estimated VOC losses [kg/y], with a representative HCOEC (Hydrocarbon Odour Emission Capacity) [ou_E/kg] value for each stored product, according to [13]:

$$\mathrm{OER}[ou_E/s] = \frac{\mathrm{HCOEC}\ [ou_E/kg] \times L_{tot}\ [kg/y]}{8760\ h/y \times 3600\ s/h} \quad (4)$$

where HCOEC is the hydrocarbon odour emission capacity and L_{tot} the yearly VOC losses.

VOC losses were derived on a monthly basis using the equations for external floating roof tanks provided in Chapter 7 of the U.S. EPA AP-42 methodology [53], accounting for all relevant loss mechanisms, including rim seal, deck fitting, and withdrawal losses. The required input parameters include tank geometric characteristics (tank diameter and height), roof and seal configuration, number and type of deck fittings, product properties, and operating conditions. Meteorological inputs required by the AP-42 equations, such as ambient temperature and wind speed, were derived from the CALMET meteorological fields used for dispersion modelling. All remaining tank-specific parameters were obtained from refinery technical databases and design documentation.

The HCOEC values were determined through laboratory analyses conducted by the Olfactometric Laboratory of Politecnico di Milano on various refinery cuts to assess their odour potential. To measure HCOEC, air is bubbled through the liquid samples in a bubbler to promote the controlled evaporation of volatile compounds. The airflow is regulated and monitored, while air samples are collected and analyzed by dynamic olfactometry to measure odour concentration. The total amount of odour released due to the evaporation of a cut over a given time period can be computed as:

$$\mathrm{Od}[ou_E] = \int_0^{t_{tot}} Q_{air} \times \mathrm{Cod}(t) \times dt \quad (5)$$

where Q_{air} represents the airflow delivered to the bubbler, Cod denotes the odour concentration measured in the collected air sample, and t_{tot} refers to the time interval.

The hydrocarbon odour emission capacity can be estimated by relating the amount of odour released to the mass evaporated during the test. Further details can be found in [14].

The choice of a monthly time frame for estimating VOC losses in EFRTs follows the methodology outlined in US-EPA AP-42 [53], with the caveat that a one-month period is considered the minimum duration for estimating emissions [54], as the equations reported in US-EPA AP-42 become increasingly uncertain over shorter time spans. Although this approach does not explicitly account for short-term (daily or hourly) variability, it is consistent with the applicability limits of the AP-42 correlations.

Moreover, OER values for EFRTs were estimated based on annual VOC losses, which were homogeneously distributed throughout the year, resulting in a constant OER value without monthly variability.

The simulation of EFRTs includes a total of 33 tanks, consisting of 9 crude oil tanks, 22 gasoline tanks, and the remainder storing kerosene and gas oil.

Table 1 presents the various HCOEC and odour concentration values considered in the study for the different stored products, as well as the total annual VOC losses for EFRTs and the total annual throughput of FRTs. The reported totals were obtained by summing the contributions of all 33 EFRT tanks and all 47 FRT tanks, respectively, while tank-specific values are provided in the Supplementary Materials.

Among the hydrocarbon products considered, the highest odour potential differs depending on tank typology. For FRTs, bitumen is characterized by the highest odour concentration at the vent, while for EFRTs, crude oil exhibits the highest HCOEC. However, the intrinsic odour potential of the stored product alone does not directly determine the emitted odour flux.

In the case of FRTs, the odour emission rate is primarily governed by tank operating conditions, as it results from the combination of the product-specific Cod and the airflow associated with tank filling operations. Consequently, peak emissions typically occur during filling events and periods of high throughput.

Conversely, for EFRTs, the odour emission rate is determined by the product-specific HCOEC in combination with VOC losses estimated through empirical correlations. Gasoline tanks are generally associated with the highest VOC losses, primarily due to the higher volatility of gasoline compared to other stored products. However, VOC losses from individual tanks are not governed by product type alone, but also by a range of tank-specific and operational parameters, and ambient temperature. As a consequence, EFRT emissions typically exhibit a seasonal pattern, with higher emission levels occurring during the warmer months, when volatilization processes are enhanced.

The vent of each FRTs was modelled as a point source emission, with a height equal to the tank roof, and a temperature assumed to be equal to the storage temperature of the tank. Storage temperatures for the different hydrocarbon cuts (typically 50–70 °C for fuel oil, 150–200 °C for bitumen, and near-ambient temperature for kerosene and diesel) were obtained directly from industrial Distributed Control System (DCS), where tank temperatures are continuously monitored by in-tank temperature sensors as part of standard operational control.

EFRTs were simulated as area source emissions, with an emission height corresponding to the top of the tank walls and a surface area corresponding to the circular area of the tank. The initial vertical dispersion coefficient, σ_{Z0}, defines the vertical extent of the puff at the point of emission. As outlined in the AERMOD User's Guide [55], σ_{Z0} is determined by dividing the vertical dimension of the emission source (i.e., its height) by a factor of 2.15 [56,57].

Additional input data related to FRTs and EFRTs are provided in the Supplementary Material.

3. Results

3.1. Annual Emission Trend

Figure 2 shows the comparison of total OER from EFRTs and FRTs, obtained by summing the contributions of all tanks, considering two approaches for estimating VOC losses: annual average and time-varying approach.

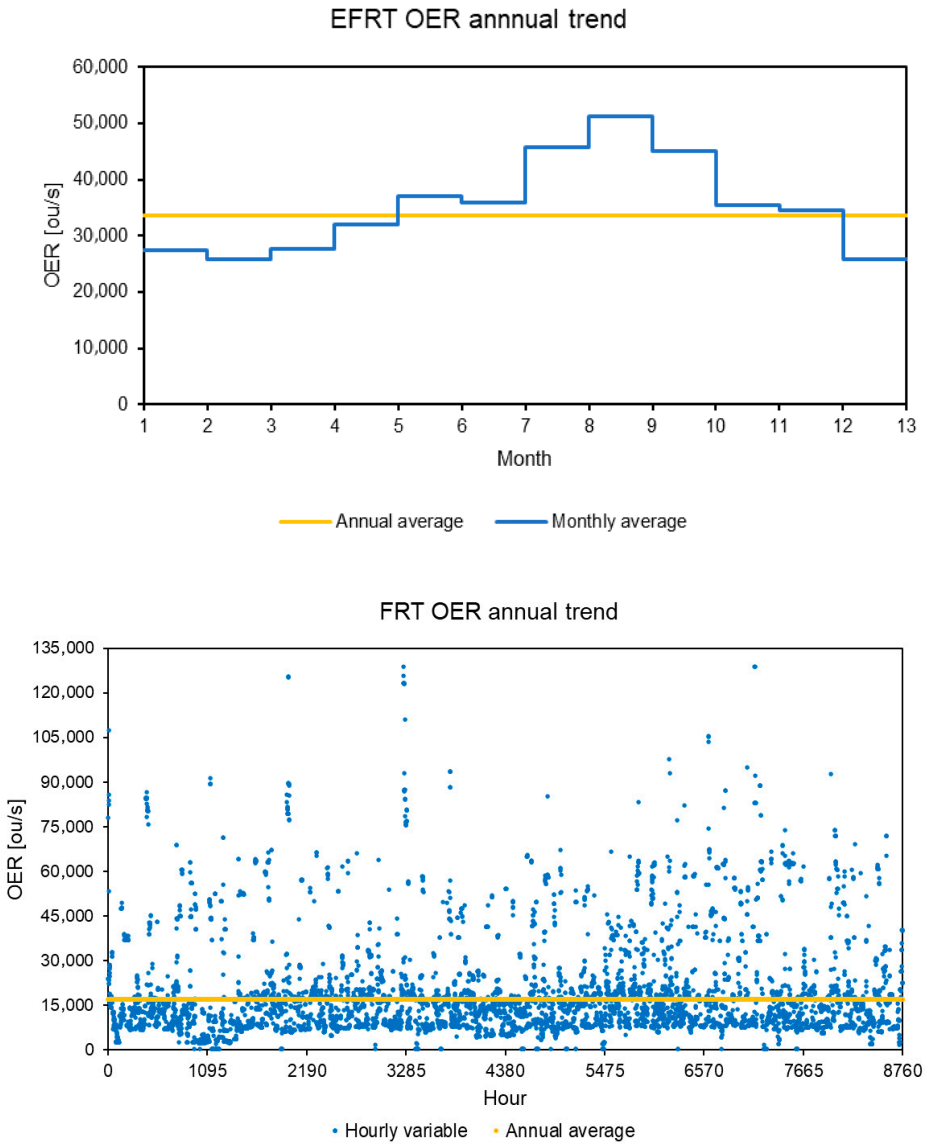

Figure 2. Annual emission trends for EFRTs and FRTs. Blue markers represent time-resolved odour emission rates (monthly for EFRTs and hourly for FRTs), while the yellow line indicates the constant annual-average emission rate used for comparison.

Concerning EFRTs, the results reveal a distinct seasonal trend, with higher VOC emissions estimated during the summer months. This increase is primarily driven by elevated ambient temperatures and enhanced solar radiation, which lead to greater VOC volatilization. Notably, the maximum deviation occurs in August, where the OER exceeds the annual trend by 50%, highlighting the potential underestimation of emission rates when relying solely on annual averages. Overall, outside the peak summer conditions, the differences between the two approaches are modest, with an average deviation of about 10%.

In the case of FRTs, Figure 2 presents a comparison of the OER estimated by summing the contributions of all tanks using the annual average throughput for each tank versus an

approach that considers hourly variations in tank levels. The results show that relying on annual averages significantly underestimates peak values, as it smooths out fluctuations driven by intense tank-filling activities or high throughput periods. Quantitatively, while the annual average OER is around 16,000 ou_E/s, the highest peaks exceed 100,000 ou_E/s, demonstrating a discrepancy of nearly one order of magnitude, corresponding to underestimations approaching 85–90% during peak emission events.

3.2. Odour Impact

Odour impact was evaluated in terms of the 98th percentile of ground-level odour concentrations over the simulation year, in accordance with the Italian regulatory framework. Hourly averaged concentration outputs (averaging time equal to 1 h) generated by CALPUFF were used as the basis for the percentile calculation.

To account for short-term concentration fluctuations relevant for odour perception, a peak-to-mean factor was applied during post-processing (using CALPOST tool, version 7.1.0). Specifically, hourly mean concentrations were multiplied by a constant peak-to-mean factor equal to 2.3, as prescribed by Italian regulation [58].

Figure 3 illustrates the direction-dependent separation distances for three reference concentration values mentioned in the recent Italian regulation for the control of odorous emissions from industrial activities [58]. According to Schauberger et al. [59], 1 ou_E/m^3 corresponds to the odour detection threshold, 3 ou_E/m^3 to odour discrimination, and 5 ou_E/m^3 to unmistakable perception. The separation distances represent contour lines (isopleths), varying according to direction, of an ambient concentration threshold. To evaluate the separation distances, a dedicated receptor nest, located at ground level, was implemented by placing receptors radially around the geometric centre of the tank area, with an angular spacing of 20° and at increasing distances from the source. For each reference concentration level, the separation distance was determined independently for each direction by interpolating between the two adjacent receptors encompassing the target concentration.

From Figure 3, it can be observed that, for EFRTs, the outcome resulting from the two different approaches for estimating odour emission fluxes is largely comparable. The separation distances highlight more significant impacts in the prevailing wind directions (NE and SW). Specifically, for angles of approximately 60° and 240° from the north, the maximum separation distance reaches 1500 m for 1 ou_E/m^3, 400 m for 3 ou_E/m^3, and 200 m for 5 ou_E/m^3. For all three reference concentration values, the separation distances estimated by the two different approaches are nearly identical, suggesting negligible differences between monthly varying emission fluxes and a constant annual emission rate.

However, in certain instances, the annual approach results in slightly higher separation distances (e.g., for 1 ou_E/m^3 at 240°), although the difference is minimal. This could be attributed to the fact that higher emission fluxes typically occur during the summer months. These months often experience conditions that favour pollutant dispersion, such as increased convective turbulence driven by higher surface temperatures. This turbulence enhances vertical mixing in the atmosphere, facilitating the dilution and transport of pollutants over greater distances. As a result, the dispersion efficiency is higher during the summer, which compensates for the elevated emission rates. Therefore, the constant annual emission rate approach may, in some cases, slightly overestimate the impacts at the 98th percentile compared to the monthly approach.

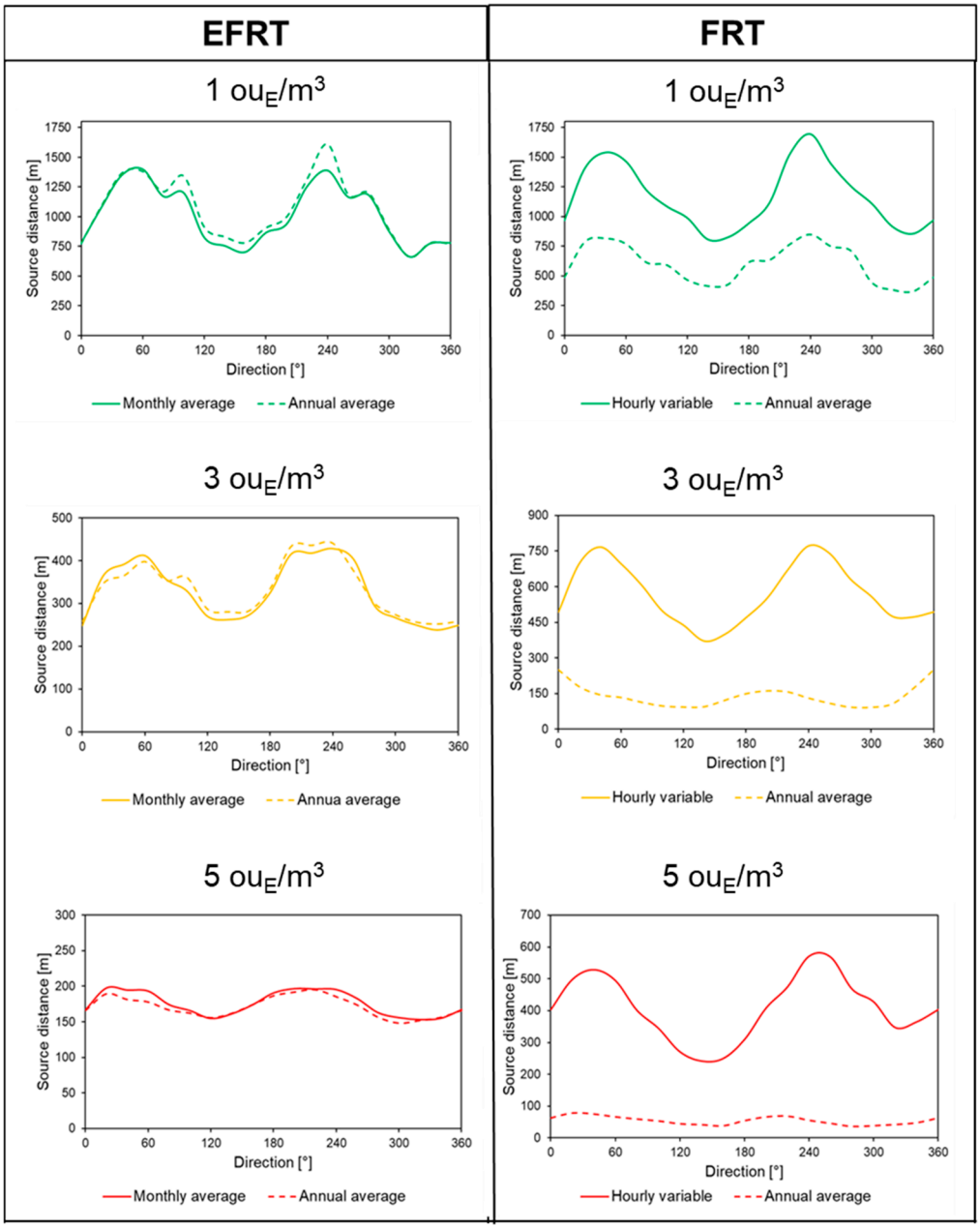

Figure 3. Separation distances referred to 1 ou$_E$/m^3, 3 ou$_E$/m^3 and 5 ou$_E$/m^3 for EFRTs and FRTs, expressed in terms of the annual 98th percentile of ground-level odour concentration.

In contrast, for FRTs, the trends in separation distances reveal more pronounced discrepancies, especially along the prevailing wind directions. Specifically, Figure 3 shows that the 1 ou$_E$/m^3 concentration isoline extends up to approximately 1500–1700 m in the NE and SW directions when hourly emission variability is considered. In contrast, using a constant annual emission rate, the same isoline is reduced to about 750 m. This trend is consistent across different concentration levels. For instance, when considering the highest reference concentration value of 5 ou$_E$/m^3, the discrepancy in separation distances reaches a factor of up to five, passing from 500 m to 100 m, highlighting the significant influence of hourly flux variability on the dispersion predictions.

Figure 4 shows the odour impact maps within the computational domain for EFRTs and FRTs obtained by the two different approaches investigated.

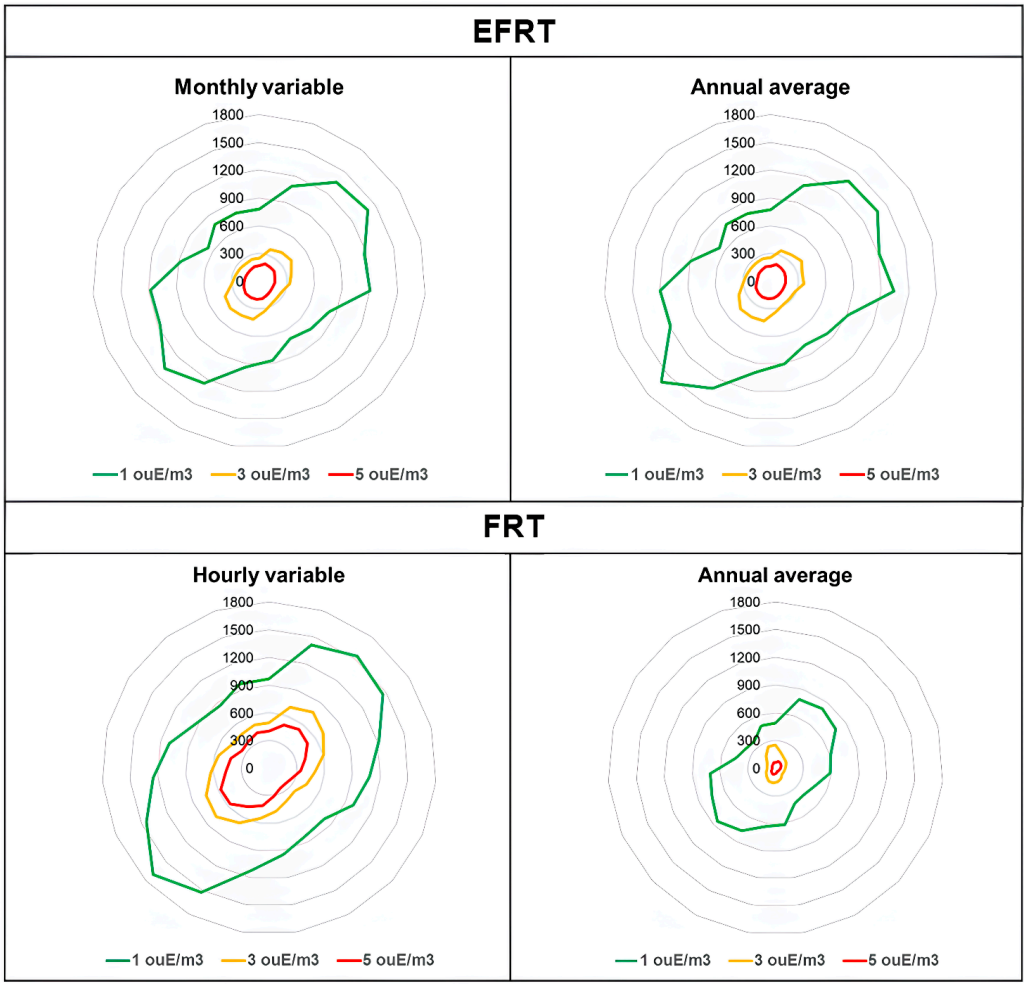

Figure 4. Odour impact maps for EFRTs and FRTs, expressed in terms of the annual 98th percentile of ground-level odour concentration.

As highlighted by the separation distances, the odour impact maps obtained for EFRTs using the two different approaches (i.e., monthly variable and annual average) appear virtually identical. In both cases, the 1 ou_E/m^3 isoline extends predominantly towards the northeast and southwest, reaching distances of up to approximately 1500 m.

In contrast, for FRTs, significant discrepancies emerge between the two simulated scenarios. When considering an hour-by-hour variable OER, the 1 ou_E/m^3 isoline reaches a maximum distance of nearly 1800 m towards the southwest. In the annual average scenario, however, the same isoline extends only up to about 900 m. Similar differences are observed for the other isolines as well.

Figure 5 highlights the relative (%) differences between the scenario with a variable OER (monthly for EFRTs and hourly for FRTs) and the scenario with an annual average approach over the simulation year:

$$\Delta\ (\%) = \frac{\left(C_{monthly/hourly} - C_{annual}\right)}{C_{annual}} \times 100 \quad (6)$$

Figure 5 shows that, in the case of EFRTs, the differences between the two emission scenarios are essentially negligible, generally falling between 5% and 10%. Specifically, positive values indicate an overprediction of the variable scenario, with deviations typically under 10%, while negative values suggest a slight underprediction of the monthly scenario, with discrepancies peaking at 15%.

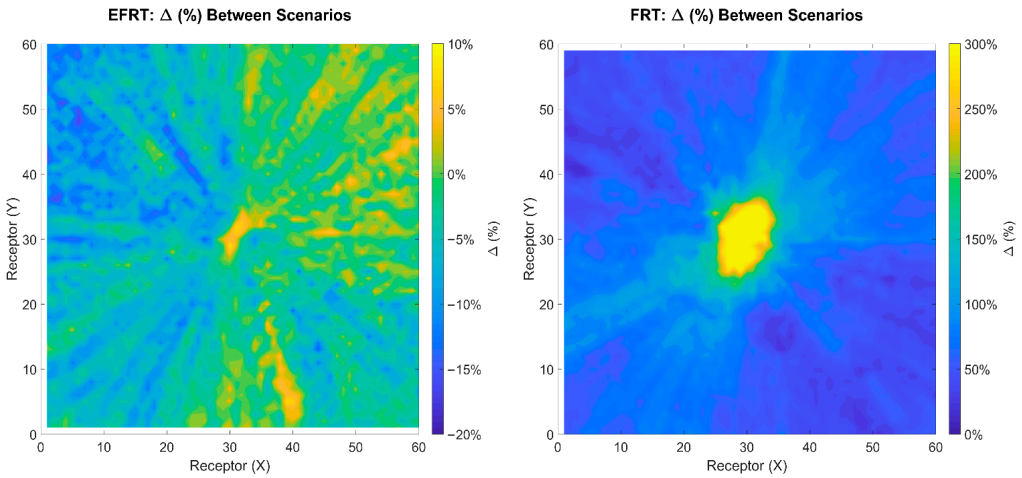

Figure 5. Relative (%) differences between the time-variable OER scenario and the annual average approach, for EFRTs and FRTs.

For FRTs, much larger differences emerge near the sources, with variations up to 300% (hourly emissions about four times higher than annual averages). At the domain boundary, discrepancies are smaller, typically 50–100% (a factor of 1.5–2). This pattern reflects dispersion dynamics: close to the source, concentrations are highly sensitive to emission temporal variability, while further away, turbulent diffusion and advection, introducing effects related to the larger-scale mixing and transport processes, reduce its influence.

In addition to the results discussed above, which refer to the Italian regulatory criterion, a supplementary analysis was carried out to investigate how the relative differences between time-resolved and annual-average emission scenarios depend on the definition of the odour impact metric. To this end, a set of alternative impact metrics representative of markedly different regulatory approaches was selected, spanning a wide range of percentile and peak-to-mean combinations. These include criteria characterized by a relatively low percentile combined with a higher peak-to-mean factor (e.g., the German reference criterion), high percentiles combined with low peak-to-mean factors (e.g., the French reference criterion), and criteria where both the percentile and the peak-to-mean factor are high (e.g., the Danish reference criterion). A criterion characterized by comparatively low values of both parameters was also considered (e.g., the Irish reference criterion).

For each impact metric, the mean percentage variation between the time-resolved and annual-average emission scenarios was calculated by averaging the relative differences over all gridded receptors within the computational domain. The results, summarized in Table 2, show a clear and systematic increase in the relative differences as the selected percentile increases. Mean variations range from approximately 36% for the 90th percentile to about 80% for the 98th percentile and increase further to 145% and 260% for the 99th and 99.5th percentiles, respectively.

Table 2. Mean relative differences (%) between time-resolved and annual-average emission scenarios for FRTs under selected odour impact metrics.

Reference Impact Metric	Peak-to-Mean	Percentile	Mean Relative Difference (%)
Germany	4	90	36
Italy	2.3	98	78
Ireland	1	98	78
Denmark	7.8	99	145
France	1	99.5	260

The comparison between the Italian and Irish reference criteria, which share the same percentile (98th) but differ in the adopted peak-to-mean factor, clearly illustrates that the peak-to-mean factor does not influence the relative differences between the two emission scenarios when applied consistently. In both cases, identical mean relative variations are obtained, confirming that the peak-to-mean factor affects absolute impact levels, while cancelling out in the computation of relative differences.

Overall, this analysis indicates that the magnitude of the differences identified for the Italian reference scenario may become even more pronounced under odour impact criteria based on higher concentration percentiles. This suggests that, in regulatory contexts adopting more stringent percentile-based metrics, the need for time-resolved emission characterizations may be even more critical in order to adequately capture short-term emission peaks and their contribution to odour impact.

4. Conclusions

This study aims to assess the impact of odour emissions from hydrocarbon storage tanks by comparing dispersion model predictions obtained using annual average emission data versus those derived from temporally resolved emission datasets.

For FRTs, the use of hourly resolved emission rates leads to substantially higher predicted odour separation distances compared to constant annual-average emissions, with discrepancies reaching up to a factor of four near the sources and remaining significant at the domain boundary. This confirms that annualized emission inputs may severely underpredict odour impacts when emissions are driven by intermittent operational activities such as tank filling. Aggregating these emissions over longer temporal scales would be expected to smooth short-term peaks and reduce the predicted impacts, potentially masking the conditions most relevant for odour nuisance.

In contrast, the analysis revealed that for EFRTs, the differences between the two approaches remain minimal, with discrepancies typically below 10%, indicating that a time-averaged approach may be adequate for this tank type within the current modelling framework. This outcome should be interpreted in light of the temporal resolution presently supported by established estimation methodologies. In particular, the monthly resolution adopted for EFRT emissions reflects the minimum time scale for which AP-42-based estimates can be considered reliable; applying the same approach at finer temporal scales would likely introduce additional uncertainty rather than improve predictive accuracy. Future research should therefore focus on the development of dedicated methods capable of resolving EFRT emissions at finer temporal resolutions, beyond the current state of the art.

Unlike traditional air pollutants, which are often regulated and evaluated based on long-term average concentrations (e.g., annual means), odour impacts are typically assessed using short-term peak concentrations and percentiles. This distinction is crucial because odour nuisance is a transient phenomenon, driven by momentary high concentrations rather than sustained exposure. Therefore, an approach that accounts for temporal emission variability is particularly relevant for odour assessments, as it better captures peak events that determine actual odour perception and potential nuisance. Furthermore, it should be noted that with higher calculation percentiles, as used in several countries [37], the differences in assessed separation distances or exposure levels increase even further compared to those based on annual mean OER.

These findings highlight the implications of emission characterization choices in odour dispersion modelling, particularly in regulatory applications, as simplified emission inputs may lead to significant underestimation of impact areas.

Future research should extend this analysis to other industrial sources, assessing whether finer temporal resolutions, such as hourly variability, provide better impact estimates than constant annual averages. For example, stack emissions, usually modelled with steady-state annual rates, may show short-term fluctuations that affect dispersion and ground-level concentrations.

Additionally, while this study considered a fixed odour concentration for FRTs based on product type, future work should investigate the influence of tank operating conditions, such as liquid level and storage temperature, on odour concentrations at the vent. Experimental studies and targeted sampling campaigns could provide valuable insights into these variations and help refine emission input data.

Moreover, extending the analysis to different meteorological conditions would be valuable, as atmospheric turbulence, wind patterns, and seasonal variability strongly affect odour dispersion and peak concentrations, thereby improving the robustness of regulatory assessments.

Supplementary Materials: The following supporting information can be downloaded at https://www.mdpi.com/article/10.3390/app16041851/s1, Supplementary Material S1: Geometry, Emission Parameters, and Elevation (MSL) data for FRTs and EFRTs.

Author Contributions: Conceptualization, F.T., M.I. and S.S.; methodology, F.T. and M.I.; software, F.T.; investigation, F.T.; data curation, F.T.; visualization, F.T.; writing—original draft, F.T.; writing—review and editing, M.I. and S.S.; supervision, M.I. All authors have read and agreed to the published version of the manuscript.

Funding: This research received no external funding.

Institutional Review Board Statement: Not applicable.

Informed Consent Statement: Not applicable.

Data Availability Statement: Dataset available on request from the authors.

Conflicts of Interest: The authors declare no conflicts of interest.

References

1. Chen, H.; Carter, K.E. Hazardous substances as the dominant non-methane volatile organic compounds with potential emissions from liquid storage tanks during well fracturing: A modeling approach. *J. Environ. Manag.* **2020**, *268*, 110715. [CrossRef] [PubMed]
2. Koçak, T.K.; Günal, A.Ç. Assessment of atmospheric volatile organic compounds at two crude oil production plants in Southeastern Türkiye. *Environ. Monit. Assess.* **2025**, *197*, 88. [CrossRef]
3. Liu, Y.; Han, F.; Liu, W.; Cui, X.; Luan, X.; Cui, Z. Process-based volatile organic compound emission inventory establishment method for the petroleum refining industry. *J. Clean Prod.* **2020**, *263*, 121609. [CrossRef]
4. Simayi, M.; Hao, Y.; Li, J.; Shi, Y.; Ren, J.; Xi, Z.; Xie, S. Historical volatile organic compounds emission performance and reduction potentials in China's petroleum refining industry. *J. Clean Prod.* **2021**, *292*, 125810. [CrossRef]
5. Rajabi, H.; Hadi Mosleh, M.; Mandal, P.; Lea-Langton, A.; Sedighi, M. Emissions of volatile organic compounds from crude oil processing—Global emission inventory and environmental release. *Sci. Total Environ.* **2020**, *727*, 138654. [CrossRef]
6. Kim, J.H.; Lee, H.E.; Yoon, S.J. Study on the speciation of VOCs at oil refining plant fenceline through active sampling. *Atmosphere* **2023**, *14*, 485. [CrossRef]
7. Gusev, A.L.; Jabbarov, T.G.; Mamedov, S.G.; Malikov, R.; Hajibalaev, N.M.; Abdullaeva, S.D.; Abbasov, N.M. Production of hydrogen and carbon in the petrochemical industry by cracking of hydrocarbons in the process of heat utilization in steel production. *Int. J. Hydrogen Energy* **2023**, *48*, 14954–14963. [CrossRef]
8. Ragothaman, A.; Anderson, W.A. Air quality impacts of petroleum refining and petrochemical industries. *Environments* **2017**, *4*, 66. [CrossRef]
9. Hini, G.; Gao, K.; Zheng, Y.; Simayi, M.; Xie, S. Emission characteristics, OFPs, and mitigation perspectives of VOCs from refining industry in China's petrochemical bases. *Aerosol Air Qual. Res.* **2023**, *23*, 220347. [CrossRef]

10. Chen, T.; Xue, L.; Zheng, P.; Zhang, Y.; Liu, Y.; Sun, J.; Han, G.; Li, H.; Zhang, X.; Li, Y.; et al. Volatile organic compounds and ozone air pollution in an oil production region in northern China. *Atmos. Chem. Phys.* **2020**, *20*, 7069–7086. [CrossRef]
11. Jindamanee, K.; Keawboonchu, J.; Pinthong, N.; Meeyai, A.; Inchai, P.; Thepanondh, S. Environmental impacts and emission profiles of volatile organic compounds from petroleum refineries. *Sci. Rep.* **2025**, *15*, 15509. [CrossRef]
12. Lv, D.; Lu, S.; He, S.; Song, K.; Shao, M.; Xie, S.; Gong, Y. Research on accounting and detection of volatile organic compounds from a typical petroleum refinery in Hebei, North China. *Chemosphere* **2021**, *281*, 130653. [CrossRef]
13. Invernizzi, M.; Sironi, S. Odour emission rate estimation methods for hydrocarbon storage tanks. *Chem. Eng. Trans.* **2021**, *85*, 67–72. [CrossRef]
14. Invernizzi, M.; Ilare, J.; Capelli, L.; Sironi, S. Proposal of a method for evaluating odour emissions from refinery storage tanks. *Chem. Eng. Trans.* **2018**, *68*, 49–54. [CrossRef]
15. Tamaddoni, M.; Sotudeh-Gharebagh, R.; Nario, S.; Hajihosseinzadeh, M.; Mostoufi, N. Experimental study of the VOC emitted from crude oil tankers. *Process Saf. Environ. Prot.* **2014**, *92*, 929–937. [CrossRef]
16. Wang, H.L.; Nie, L.; Li, J.; Wang, Y.F.; Wang, G.; Wang, J.H.; Hao, Z.P. Characterization and assessment of volatile organic compounds emissions from typical industries. *Chin. Sci. Bull.* **2013**, *58*, 724–730. [CrossRef]
17. Matsumoto, N.; Elder, M.; Ogihara, A. Japan's policy to reduce emissions of volatile organic compounds: Factors that facilitate industry participation in voluntary actions. *J. Clean Prod.* **2015**, *93*, 931–943. [CrossRef]
18. Saikomol, S.; Thepanondh, S.; Laowagul, W. Emission losses and dispersion of volatile organic compounds from tank farm of petroleum refinery complex. *J. Environ. Health Sci. Eng.* **2019**, *17*, 561–570. [CrossRef]
19. Wei, W.; Cheng, S.; Li, G.; Wang, G.; Wang, H. Characteristics of volatile organic compounds emitted from a petroleum refinery in Beijing, China. *Atmos. Environ.* **2014**, *89*, 358–366. [CrossRef]
20. Farzaneh-Gord, M.; Nabati, A.; Rasekh, A.; Saadat-Targhi, M. The effect of crude oil type on evaporation loss from Khark Island storage tanks. *Pet. Sci. Technol.* **2013**, *31*, 866–879. [CrossRef]
21. Rota, R.; Frattini, S.; Astori, S.; Paludetto, R. Emissions from fixed-roof storage tanks: Modeling and experiments. *Ind. Eng. Chem. Res.* **2001**, *40*, 5847–5857. [CrossRef]
22. Maxwell, A.; Lawal, A. Petroleum product storage tank, design and loss control management. In Proceedings of the SPE African Health, Safety, Security, Environment, and Social Responsibility Conference and Exhibition, Accra, Ghana, 4–6 October 2016.
23. Zinke, R.; Köhler, F.; Krause, U. Long-term emission measurements at a floating roof tank for gasoline storage. *J. Loss Prev. Process Ind.* **2018**, *55*, 152–161. [CrossRef]
24. Mansour, E.M.; El Aily, M.; Desouky, S.M. Flashing losses emission evaluation from crude oil storage tank. *Egypt. J. Chem.* **2020**, *63*, 4457–4462. [CrossRef]
25. Wang, Y.; Liu, M.; Liu, F.; Zhao, C.; Zhao, D.; Han, F.; Liu, C. Research on the effect of wall corrosion and rim seal on the withdrawal loss for a floating roof tank. *Environ. Sci. Pollut. Res.* **2018**, *25*, 18434–18442. [CrossRef]
26. Howari, F.M. Evaporation losses and dispersion of volatile organic compounds from tank farms. *Environ. Monit. Assess.* **2015**, *187*, 256. [CrossRef]
27. Jovanovic, J.; Jovanovic, M.; Jovanovic, A.; Marinovic, V. Introduction of cleaner production in the tank farm of the Pancevo Oil Refinery, Serbia. *J. Clean Prod.* **2010**, *18*, 791–798. [CrossRef]
28. Lu, C.; Huang, H.; Chang, S.; Hsu, S. Emission characteristics of VOCs from three fixed-roof p-xylene liquid storage tanks. *Environ. Monit. Assess.* **2013**, *185*, 6819–6830. [CrossRef] [PubMed]
29. Saikomol, S.; Thepanondh, S.; Laowagul, W.; Malakan, W.; Keawboonchu, J.; Kultan, V. Characteristics and dispersion modeling of VOCs emission released from the tank farm of petroleum refinery complex. *EnvironmentAsia* **2021**, *14*, 1–12. [CrossRef]
30. Yang, H.; Ren, B.; Huang, Y.; Zhang, Z.; Hu, W.; Liu, M.; Zhao, H.; Jiang, G.; Hao, Z. Volatile organic compounds emissions from internal floating-roof tank in oil depots in Beijing: Influencing factors and emission reduction strategies analysis. *Sci. Total Environ.* **2024**, *916*, 170222. [CrossRef] [PubMed]
31. Barbeş, S.B.; Badea, A.C.; Iordache, V. Volatile organic compounds losses simulation during storage of gasoline. *IOP Conf. Ser. Earth Environ. Sci.* **2023**, *1185*, 012009. [CrossRef]
32. Mott, A.; Guo, H. Odour dispersion modelling, impact criteria, and setback distances for an oil refinery plant. *Atmos. Environ.* **2022**, *270*, 118879. [CrossRef]
33. Motalebi Damuchali, A.; Guo, H. Developing an odour emission factor for an oil refinery plant using reverse dispersion modeling. *Atmos. Environ.* **2020**, *222*, 117167. [CrossRef]
34. Motalebi Damuchali, A.; Guo, H. Evaluation of odour properties, their relationships, and impact of an oil refinery plant on the surrounding environment using field measurements. *Atmos. Environ.* **2020**, *230*, 117480. [CrossRef]
35. Santos, J.M.; Griffiths, R.F.; Roberts, I.D.; Reis, N.C. A field experiment on turbulent concentration fluctuations of an atmospheric tracer gas in the vicinity of a complex-shaped building. *Atmos. Environ.* **2005**, *39*, 4999–5012. [CrossRef]
36. Bokowa, A.; Diaz, C.; Koziel, J.A.; McGinley, M.; Barclay, J.; Schauberger, G.; Guillot, J.M.; Sneath, R.; Capelli, L.; Zorich, V.; et al. Summary and overview of the odour regulations worldwide. *Atmosphere* **2021**, *12*, 206. [CrossRef]

37. Brancher, M.; Piringer, M.; Grauer, A.F.; Schauberger, G. Do odour impact criteria of different jurisdictions ensure analogous separation distances for an equivalent level of protection? *J. Environ. Manag.* **2019**, *240*, 394–403. [CrossRef]
38. Brancher, M.; Knauder, W.; Piringer, M.; Schauberger, G. Temporal variability in odour emissions: To what extent this matters for the assessment of annoyance using dispersion modelling. *Atmos. Environ. X* **2020**, *5*, 100054. [CrossRef]
39. Zhang, Q.; Zhou, X. Assessing peak-to-mean ratios of odour intensity in the atmosphere near swine operations. *Atmosphere* **2020**, *11*, 224. [CrossRef]
40. Ghannam, K.; El-Fadel, M. Emissions characterization and regulatory compliance at an industrial complex: An integrated MM5/CALPUFF approach. *Atmos. Environ.* **2013**, *69*, 156–169. [CrossRef]
41. Varela-Bruce, C.; Antileo, C. Assessment of odour emissions by the use of a dispersion model in the context of the proposed new law in Chile. *J. Environ. Manag.* **2021**, *295*, 113208. [CrossRef]
42. Emert, A.D.; Griffis-Kyle, K.; Portillo-Quintero, C.; Smith, P.N. USEPA CALPUFF validation and dispersion modeling of beef cattle feedlot PM_{10} and $PM_{2.5}$ emissions factors. *Atmos. Environ.* **2024**, *316*, 120189. [CrossRef]
43. Jittra, N.; Pinthong, N.; Thepanondh, S. Performance evaluation of AERMOD and CALPUFF air dispersion models in industrial complex area. *Air Soil Water Res.* **2015**, *8*, 87–95. [CrossRef]
44. Tagliaferri, F.; Facagni, L.; Invernizzi, M.; Sironi, S. Variability in odour impact assessment due to different cloud cover estimation approaches: A northern Italy case study. *Case Stud. Chem. Environ. Eng.* **2023**, *8*, 100492. [CrossRef]
45. Tagliaferri, F.; Facagni, L.; Invernizzi, M.; Ferrer Hernández, A.L.; Hernández-Garces, A.; Sironi, S. Odor impact assessment via dispersion model: Comparison of different input meteorological datasets. *Appl. Sci.* **2024**, *14*, 2457. [CrossRef]
46. Tagliaferri, F.; Invernizzi, M.; Sironi, S. Strategies for the reduction of odour impact via dispersion modelling: A case study of a rendering plant. *Chem. Eng. Trans.* **2024**, *112*, 181–186. [CrossRef]
47. Szalata, L.; Zwózdziak, J.; Majerník, M.; Cierniak-Emerych, A.; Jarossová, M.A.; Dziuba, S.; Knošková, L.; Drábik, P. Assessment of the odour quality of the air surrounding a landfill site: A case study. *Sustainability* **2021**, *13*, 1713. [CrossRef]
48. Yaacof, N.; Qamaruz Zaman, N.; Yusup, Y.; Yusoff, S. Establishment of suitable separation distance by using different methods for malodor mitigation from palm oil mill. *Environ. Sci. Pollut. Res.* **2019**, *26*, 24286–24299. [CrossRef]
49. Brancher, M.; Hoinaski, L.; Piringer, M.; Prata, A.A.; Schauberger, G. Dispersion modelling of environmental odours using hourly-resolved emission scenarios: Implications for impact assessments. *Atmos. Environ. X* **2021**, *12*, 100124. [CrossRef]
50. Schauberger, G.; Piringer, M.; Petz, E. Influence of the variability of the odour emission rate on the separation distance shown for the Irish odour impact criterion. *Chem. Eng. Trans.* **2016**, *54*, 193–198. [CrossRef]
51. Scire, J.S.; Strimaitis, D.G.; Yamartino, R.J. *A User's Guide for the CALPUFF Dispersion Model*; Earth Tech. Inc.: Concord, MA, USA, 2000.
52. Scire, J.; Robe, F.; Fernau, M.; Yamartino, R. *A User's Guide for the CALMET Meteorological Model*; Earth Tech. Inc.: Concord, MA, USA, 2000.
53. Van Harreveld, A.P. Update on the new EN 13725:2021. *Chem. Eng. Trans.* **2021**, *85*, 115–120. [CrossRef]
54. U.S. EPA. *Emission Factor Documentation for AP-42 Organic Liquid Storage Tanks*; U.S. Environmental Protection Agency: Durham, NC, USA, 1997.
55. U.S. EPA. *User's Guide for the AMS/EPA Regulatory Model (AERMOD)*; EPA-454/B-18-001; U.S. Environmental Protection Agency: Durham, NC, USA, 2018.
56. Hartley, S.; Rosenbaum, A.; Holder, C.; Cohen, J.; Graham, S.; Brode, R.; Thurman, J.; Langstaff, J.; Fox, T. Application of AERMOD to Region-wide Emissions in an Urban Setting in Support of the NO_2 NAAQS Review. In Proceedings of the AWMA Guideline on Air Quality Models: Next Generation of Models, Raleigh, NC, USA, 26–30 October 2009. [CrossRef]
57. Warren, C.J.; Paine, R.J.; Connors, J.A.; Szembek, C.; Knipping, E. Evaluation of a revised AERMOD treatment of plume dispersion in the daytime elevated stable layer. *Air Waste Manag. Assoc.* **2022**, *72*, 1040–1052. [CrossRef] [PubMed]
58. Ministero dell'Ambiente e della Sicurezza Energetica. *Decreto Direttoriale 28 Giugno 2023, n. 309*; Ministero dell'Ambiente e della Sicurezza Energetica: Rome, Italy, 2023.
59. Schauberger, G.; Piringer, M.; Petz, E. Diurnal and annual variation of the sensation distance of odour emitted by livestock buildings calculated by the Austrian odour dispersion model. *Atmos. Environ.* **2000**, *34*, 4839–4851. [CrossRef]